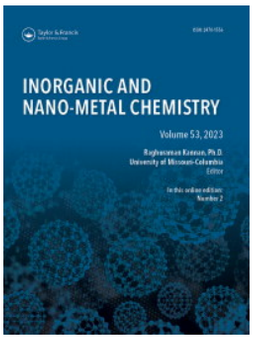

Taylor & Francis
Taylor & Francis Group

Inorganic and Nano-Metal Chemistry

ISSN: (Print) (Online) Journal homepage: https://www.tandfonline.com/loi/lsrt21

Radio-sensitivity on MCF-7 cells of silver nanoparticles synthesized by *Silybum marianum*

Erdi Bilgic, Nina Tuncel & Timur Koca

To cite this article: Erdi Bilgic, Nina Tuncel & Timur Koca (2023) Radio-sensitivity on MCF-7 cells of silver nanoparticles synthesized by *Silybum marianum*, Inorganic and Nano-Metal Chemistry, 53:2, 122-130, DOI: 10.1080/24701556.2021.1987460

To link to this article: https://doi.org/10.1080/24701556.2021.1987460

INORGANIC AND NANO-METAL CHEMISTRY
2023, VOL. 53, NO. 2, 122–130
https://doi.org/10.1080/24701556.2021.1987460

Radio-sensitivity on MCF-7 cells of silver nanoparticles synthesized by *Silybum marianum*

Erdi Bilgic[a], Nina Tuncel[b,c], and Timur Koca[d]

[a]Vocational School of Health Sciences, Department of Medical Services and Techniques, Istanbul Gelisim University, Istanbul, Turkey; [b]Faculty of Science, Department of Physics, Akdeniz University, Antalya, Turkey; [c]Faculty of Medicine, Department of Radiation Oncology, Akdeniz University, Antalya, Turkey; [d]Faculty of Medicine, Department of Radiation Oncology, Akdeniz University, Antalya, Turkey

ABSTRACT

In the green synthesis method, various plants gain importance due to the synergistic effect created by their rich phytochemical properties. In this study, SM (thistle-*Silybum marianum*) plant, which is known with its antioxidant and anticarcinogenic properties in the literature, forms the source of motivation. Silver nanoparticles (Ag NPs) were synthesized in SM aqueous extracts by this method. The formation of Ag NPs was confirmed by transmission electron microscopy (TEM), UV-Vis and XRD spectrophotometers. Cytotoxicity of MCF-7 cells, incubated for 24 and 48 hours with different mass concentrations of Ag NPs, was determined by MTT test. Additionally, in this study, the radio-sensitizing effects of Ag NPs synthesized via SM seeds were investigated for the first time. Moreover, MCF-7 cells incubated with Ag NPs for 1-2 and 4 hours were exposed to 6 MV energy X-ray radiation.

ARTICLE HISTORY
Received 10 March 2021
Accepted 29 August 2021

KEYWORDS
Silybum marianum; Silver Nanoparticles; MCF-7; MTT; Radio-sensitivity

Introduction

The synthesis methods of nanostructures include physical, chemical and biological approaches. Among these methods, biological methods have been preferred in recent years due to its environmental friendliness and being economic. While physical methods such as vapor condensation and molecular beam enlargement (Molecular Beam Epitaxy, MBE) [1] require extremely expensive technological tools and equipment, almost none of them are suitable for public production. Although chemical methods[2] are suitable for cheap public production compared to physical methods, the toxic chemicals used are extremely harmful to the environment. Biological methods are environmentally friendly, as they use bacteria,[3] yeast[4] and plants.[5]

Ag NPs synthesized in studies using plants such as *Juglans regia,*[5] *Hypericum perforatum,*[6] *Hydnocarpus pentandra,*[7] and *Prosopis juliflora*[8] have been investigated effects on against bacteria such as *S. aureus, E. faecalis, E. coli, S. typhi* and *P. aeruginosa.*[9] Most of these studies focus on how antibacterial activity is affected by parameters such as nanoparticle size, concentration and synthesis method.

Krishnaraj et al.[10] synthesized Ag NPs in *Acalypha indica* leaf extracts. They investigated the antibacterial effects of the colloidal Ag NPs they synthesized on Escherichia coli and *Vibrio cholerae* cells. They emphasized that it acts against these bacteria at concentrations of minimum 10 μg/ml.

Similarly, in another study Nabikhan et al.[11] the antibacterial activities of Ag NPs synthesized in *Sesuvium portulacastrum* extracts against *Pseudomonas aeruginosa, Staphylococcus aureus, Listeria monocytogenes, Micrococcus luteu* and *Klebsiella pneumoniae* human pathogens were investigated. In the study, the crystal structures of Ag NPs in sizes varying between 5-20 nm were examined and the emphasis was placed on the concentration dependent antibacterial activity.

Antimicrobial effects of Ag NPs are also being investigated. In recent years Ag NPs has begun to be investigated on viruses such as HIV-1,[12,13] hepatitis B,[14] herpes simplex,[15] respiratory syncytial,[16] monkey flower,[17] Tacaribe,[18] H1N1 influenza A virus.[19,20]

Lara et al.[21] showed in their study that Ag NPs they took in non-cytotoxic concentrations exerted anti-HIV activity at an early stage of viral replication, most likely as an inhibitor of viral entry. In addition, they showed that Ag NPs bind to gp120, thus preventing CD4-dependent virion binding, fusion and infectivity, acting as an effective virucidal agent against the virus. They also emphasized that Ag NPs inhibit the post-entry stages of the HIV-1 life cycle.

Apart from these, there are studies investigating the effects of Ag NPs on cancer cells. Most of these studies deal with the cytotoxicity and radio-sensitizing effects of Ag NPs.

In literature studies on cytotoxicity studies, Ag NPs; many cell lines have been focused on such as A549,[22] HepG2,[23] MCF-7,[24] HeLa and U937.[25] Similar aspects of these studies include investigating the concentration-dependent cytotoxicity of nanoparticles used at different concentrations and determining their IC50 concentrations. Apart

CONTACT Nina Tuncel ninatuncel@gmail.com Akdeniz University, Antalya, Turkey
Biographical notes: This study was produced from the PhD thesis of Erdi Bilgiç, a student of Akdeniz University Institute of Science.

from this, there are studies indicating that the sizes of Ag NPs affect their cytotoxicity.[24–28]

Researches need to be improved due to the limited number of these studies, the different phytochemicals in the plant content, and the peculiar characteristics of nanoparticles. There are also limited studies on the cytotoxic effects of bio-synthesized Ag NPs against cancer cell lines.

For the green synthesis of Ag NPs, synthesis and characterization of Ag NPs using SM seed extract have been reported in various reports.[29] SM, is a plant of the *Asteraceae* family that bears pale green leaves with purple flowers and some hibiscus spines. The extract obtained from SM seeds contains 65–80% silymarin (Flavonolignan complex), 20–25% fatty acids, a small amount of flavonoid (taxifoline) and other polyphenolic compounds.[30] The major bioreactive components in SM are flavonolignae including silyl A, silibin B, isocylbin A, isosylbin B, silydianine and silicristine.[31] The phytochemicals contained in this plant have been investigated in medical fields for years.[32]

The antioxidant activities of SM on mammalian cells are promising and there are studies showing that it has a repair effect on tissues and organs directly affected by drug cytotoxicity such as liver. In a study by Flora et al.,[32] they stated that SM causes the displacement of toxins bound to the liver and rapid regeneration of liver cells (Flora et al., 1998). Fanoudi et al.[33] also defined SM as a natural antidote against natural and chemical toxicities. Besides, Tzeng et al.[34] stated that silymarin, a phytochemical contained in SM, reduced connective tissue growth factor to treat liver fibrosis in mice treated with carbon tetrachloride. In another study, Shaker et al.[35] investigated the antiradical and anticarcinogenic roles of silymarin. In the study, they stated that by increasing the antioxidant ability of hepatocytes with phytochemicals such as silymarin, oxidative/nitrosative stress can be resisted and the progression of liver disease can be prevented. Moreover, they said that the increasing demand for natural plant products could replace biologically harmful molecules with their antioxidant potential.

It has also been shown that silymarin may be useful in reducing the likelihood of some types of cancer. Bhatia et al.[36] investigated the chemo-preventive and anti-carcinogenic effects of SM and suggested that silymarin, the main component of SM, has chemo-preventive and anti-carcinogenic effects.

In many studies, the green synthesis method, which uses the leaves, seeds, fruits, roots and stems of plants as reducing and encapsulating agents, has been preferred. The phytochemicals contained in the plants used in the synthesis process in this method have been investigated for years in drug studies. The synergetic effect created by these phytochemicals is the motivation for this study. Therefore, milk thistle seed was preferred for the synthesis of Ag NPs in the synthesis processes. In addition, the ability of metal nanoparticles synthesized by this method to eliminate toxic by-products that may be harmful to both the environment and human health has been another source of motivation.

Materials and methods

Preparation of plant extracts

SM seeds were added to 100 ml distilled water 5,000 g and mixed in magnetic stirrer at 90 °C for 30 minutes. After resting for 10 minutes, SM extract was prepared by passing through filter paper.

UV-Vis spectroscopy and nanoparticle images

The prepared plant extracts and 4 mM, 2 mM and 1 mM $AgNO_3$ solutions dissolved in distilled water were mixed in the dark at a ratio of 1:1. After a 24-hour reduction period, absorbance spectra were obtained by purchasing services from Yı ldı z Technical University Central Laboratories in the range of 300–800 nm with 0.5 nm steps in a PGENERAL-T80 + brand/model UV-Vis spectrophotometer.

To obtain TEM images, the nanoparticles synthesized in the extract-$AgNO_3$ mixture were taken with a micropipette and dropped on the grid. After waiting for 3 days, an appointment was made to receive TEM images, considering it was dry. TEM images were obtained by purchasing services from Eskişehir Osman Gazi University Central Research Laboratory Application and Research Center (ARUM). Carbon grids were used while taking TEM images. Images were obtained at 100 kV energy, with 40000-215600 times magnification.

X-Ray diffractometer (XRD)

Colloidal nanoparticles obtained with SM were dried in an oven at 300 C for 3 days. During the drying process, the nanoparticle solution was made ultrasonic bath for 30 minutes once a day. The dried Ag NPs were delivered in the YTU central laboratory, where the service was purchased, for XRD results.

Cell cultures and MTT viability tests

108, 80, 40, 20, 10, 5, 0 µg/ml at mass concentrations and 5 ml samples were obtained for MTT viability tests. There is no Ag NP at a concentration of 0 µg/ml and the extract was diluted 1:1 with distilled water. The prepared samples were used in the MTT test and 100 µl of each sample was taken and cytotoxicity tests were performed.

The MCF-7 cell line was seeded in a 96-well plate at 105 cells/ml per well. Cells were allowed to hold in the incubator with 37 °C CO_2 for 24 hours. At the end of 24 hours, the samples were planted in the wells in 3 repetitions. After the samples were exposed to cells in the wells for 24 hours, MTT viability test was performed. DMSO solution was used as positive control and DMEM medium only as negative control. Photometric reading: done at 570 nm. The results calculated as the negative control were considered 100% alive.

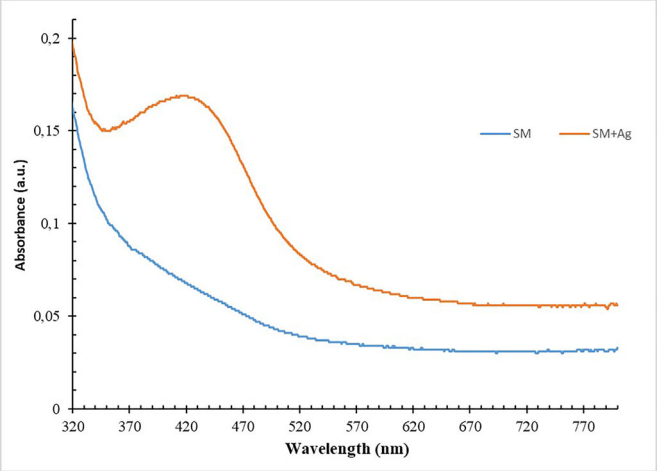

Figure 1. UV-Vis absorbance spectra of Ag NPs synthesized with 4 mM $AgNO_3$ in milk thistle seed extract.

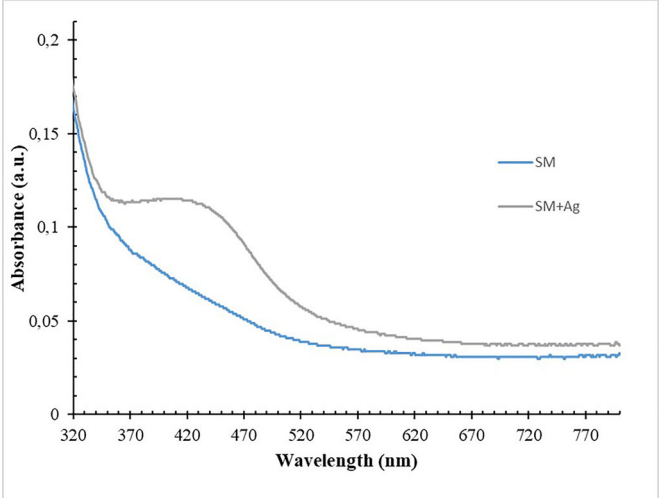

Figure 3. UV-Vis absorbance spectra of Ag NPs synthesized with 2 mM $AgNO_3$ in milk thistle seed extract.

Figure 2. Ag NPs synthesized with 4 mM $AgNO_3$ in milk thistle seed extract.

Figure 4. Ag NPs synthesized with 2 mM $AgNO_3$ in milk thistle seed extract.

Radio-Sensitizing effects

MCF-7 cells were grown in DMEM medium with 10% Fetal bovine serum, penicillin, L-glutamine and streptomycin. ELEKTA brand linear accelerator (LINAC) device that produces 6 MV X-rays was used. The application was made by taking 15 × 15 cm area size and 80 cm SSD. MCF-7 cells incubated for 1, 2 and 4 hours with 100 µg Ag NPs at IC50 concentrations were irradiated with a bolus of 6 Gy ionizing radiation in 96-well plates at 1 Gy/min. It was obtained by adding 100 µl distilled water to MCF-7 cells taken as the control group. For the radio-susceptibility of the plant extracts, 100 µl of 1:1 diluted extract was incubated. Similar experimental processes have been applied for nanoparticles obtained from each plant extract.

Results

UV-Vis spectroscopy and nanoparticle images

UV-Vis measurements contain information about the presence of the nanoparticles, their approximate size and shape. Characteristic plasmon band formation related to the shape and size distribution of nanoparticles is observed with UV-Vis measurements.

Absorbance spectra of $AgNO_3$ added plant extract (nanoparticle solution) and only plant extract relative to distilled water were taken. The peak positions of UV-Vis spectra given in Figures 1–6 are given in Table 1.

To obtain TEM images, the nanoparticles synthesized in the extract-$AgNO_3$ mixture were taken with a micropipette and dropped on the grid. After waiting for 3 days, an appointment was made to receive TEM images, considering it was dry. TEM images were obtained by purchasing services from Eskişehir Osman Gazi University Central Research Laboratory Application and Research Center (ARUM).

It was observed that the nanoparticles synthesized through TEM images have a spherical shape (Figures 7–9). Nanoparticle sizes exhibited different size distributions according to the plant and $AgNO_3$ concentration in which it was synthesized (Table 1).

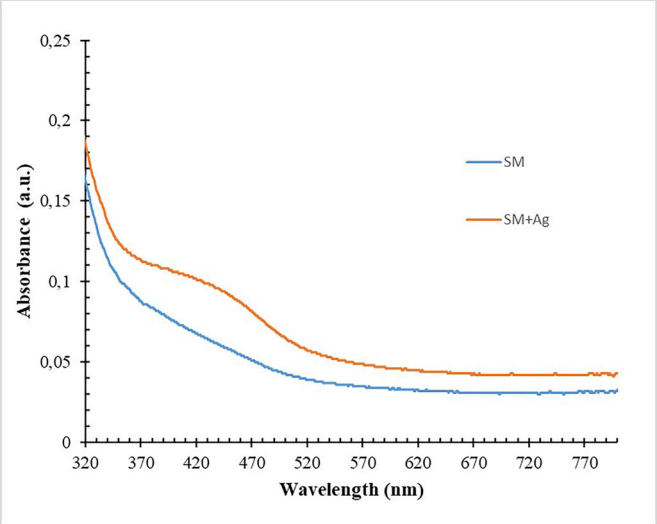

Figure 5. UV-Vis absorbance spectra of Ag NPs synthesized with 1 mM $AgNO_3$ in milk thistle seed extract.

Figure 6. Ag NPs synthesized with 1 mM $AgNO_3$ in milk thistle seed extract.

Table 1. Peak positions of UV-Vis spectra of synthesized Ag NPs and their average sizes belong to TEM images.

$AgNO_3$ Molarity (mM)	Peak Locations (nm)	Average Size (nm)
1	391,5 ± 3,5	2,5 ± 1
2	402,5 ± 9,5	8 ± 7
4	417,5 ± 4,0	13,5 ± 8,5

X-Ray diffractometer (XRD)

Ag NPs synthesized in plant extracts were dried for XRD analysis. The dried Ag NPs were sent to Yıldız Technical University for XRD analysis. XRD graphics of Ag NPs synthesized in different $AgNO_3$ molar concentrations in thistle seed extracts are shared. According to the XRD data (111), (200), (220) and (311) surface-centered cubic structures of the surfaces were determined (Figure 10–12). These values are shared in Table 2.

Cell cultures and MTT viability test

As given in Figure 13, it has been observed that cell viability decreases with the mass concentrations of Ag NPs.

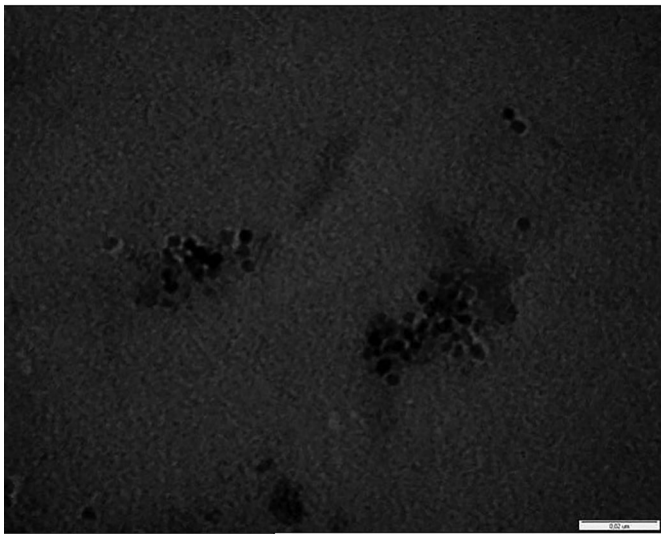

Figure 7. TEM image of Ag NPs synthesized with 4 mM $AgNO_3$ in milk thistle seed extract.

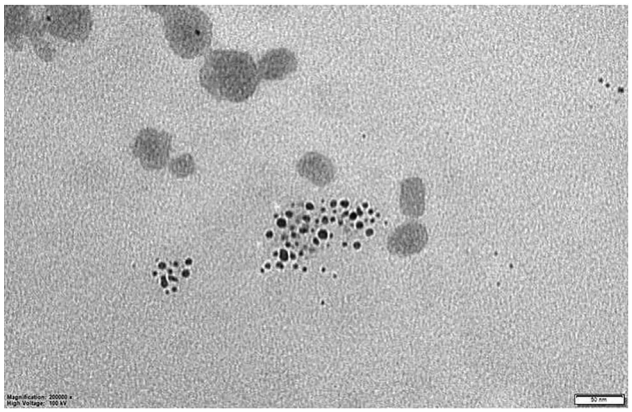

Figure 8. TEM image Ag NPs synthesized with 2 mM $AgNO_3$ in milk thistle seed extract.

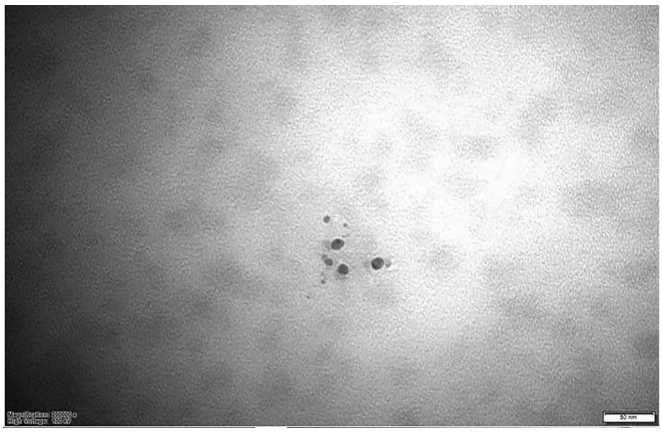

Figure 9. TEM image Ag NPs synthesized with 1 mM $AgNO_3$ in milk thistle seed extract.

According to MTT results IC50 values were calculated as 42 µg/ml at the end of the 24-hour incubation period and 38 µg/ml after the 48-hour incubation period.

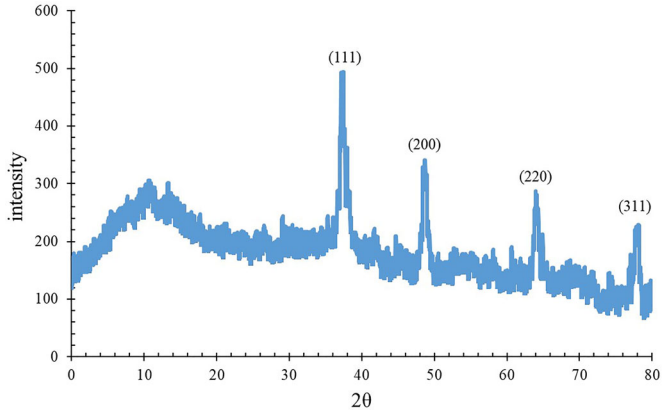

Figure 10. XRD pattern of Ag NPs synthesized with 4 mM $AgNO_3$ in milk thistle seed extract.

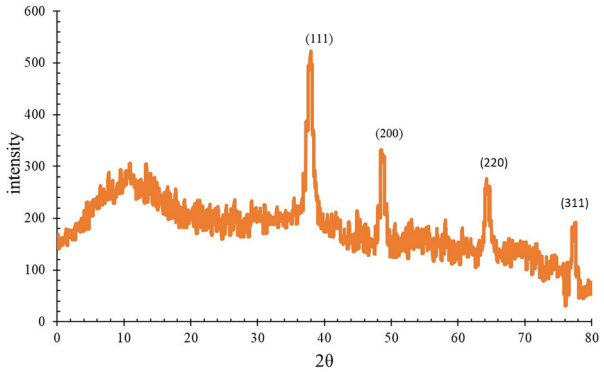

Figure 11. XRD pattern of Ag NPs synthesized with 2 mM $AgNO_3$ in milk thistle seed extract.

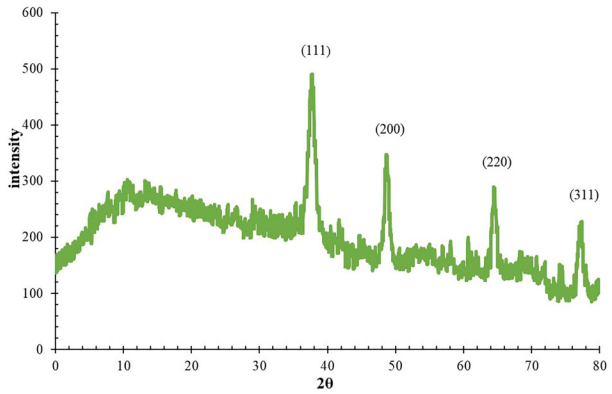

Figure 12. XRD pattern of Ag NPs synthesized with 1 mM $AgNO_3$ in milk thistle seed extract.

Radio-sensitizing effects

For the radiation studies, a radiation dose of 6 Gy was applied in a single fraction using 6 MV energy X-rays to MCF-7 cells incubated with Ag NPs, whose IC50 doses were determined as 42 µg/ml.

As shown in Figure 14, cell viability of nanoparticles synthesized in milk thistle seed extract without radiation was found to be 54.8% and cell viability was 60.2% when only radiation was applied. Cell viability of the irradiated MCF-7 cells after incubation with Ag NPs for different times was respectively obtained as 25.3%; 8.4%; and 15.8% after 1, 2 and 4 hours of incubation.

Table 2. 2θ values indicating the crystal structure of nanoparticles according to plant species.

Ag Molar Concentration (mM)	2d			
	(111)	(200)	(220)	(311)
1	37,76	44,72	64,42	77,36
2	37,96	44,52	64,24	77,60
4	37,48	44,60	63,98	78,16

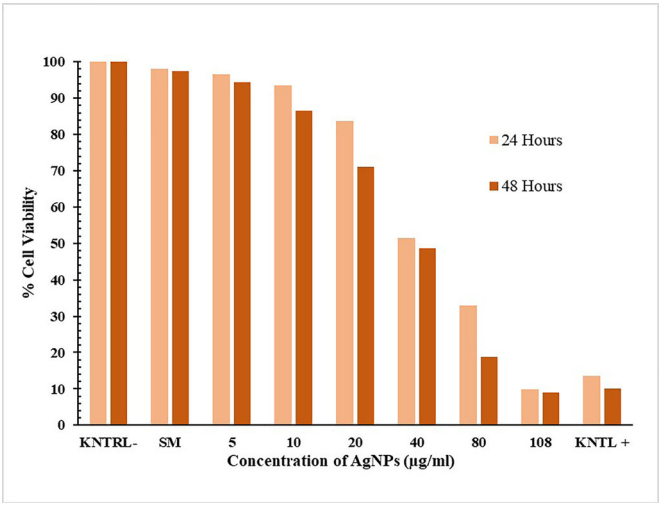

Figure 13. MTT-assay for Ag NPs treated MCF7 cells.

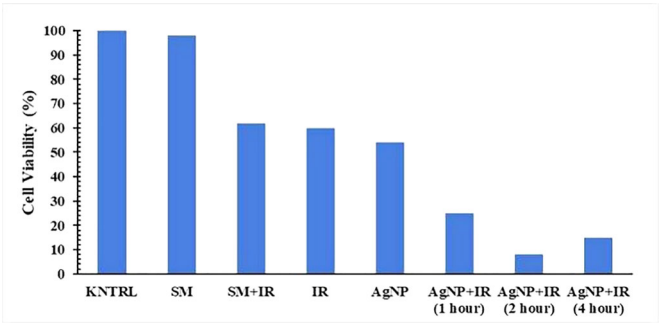

Figure 14. Radio-sensitizing effect of Ag NPs on MCF-7 cells.

Discussion

UV-Vis spectroscopy and nanoparticle images

UV-Vis spectroscopy is an important technique for determining the development and stability of nanoparticles. Colloidal solutions of Ag NPs are often intensely colored due to surface plasmon resonance (SPR) resulting from the collective emission of free conduction electrons in the gas phase of the particles.[37] According to Sharma et al.,[38] solutions containing colloidal nanoparticles smaller than the wavelength of visible light are yellow in color and when looking at studies in general, it has been noted that Ag NPs

form surface plasmon bands in the 350-450 nm range.[5,7,8,39,40]

Before proceeding to morphological investigations in nanoparticle synthesis, the nanoparticle colloidal solution should be standardized with UV-Vis spectrophometry. Kumar and Yadav[41] stated that nanoparticles give their characteristic absorption peaks, and with this feature, nanoparticles can be monitored and Ag NPs give an absorption peak around 450 nm. Mie[42] states that as the average size of nanoparticles with the same shape increases, the peak maximums will be observed at longer wavelengths. SPR bands are also related to the morphology of Ag NPs. He et al.[43] stated that the presence of a single SPR peak in the colloidal solutions of Ag NPs indicates that the shapes of Ag NPs are spherical.

In this study, UV-Vis spectra of Ag NPs synthesized with milk thistle seeds were scanned in the range of 300-800 nm at 0.5 step intervals. In the absorbance spectra taken 24 hours after $AgNO_3$ was added to the plant extracts, it was observed that the peak maxima varied between 391.5-423.5 nm. In all of the integrated Ag NPs; there is a redshift in the positions of the absorbance peaks associated with $AgNO_3$ molar concentrations. As reported by Mie,[42] as the average diameters of nanoparticles with the same shape increase, their peak maximums are observed at longer wavelengths. In other words, as the average diameters of nanoparticles increase, their peak maximum shifts to red. In addition, He et al.[43] stated that the presence of a single peak maximum in absorbance spectra contains information that nanoparticle sizes may be spherical. As such, UV-Vis measurements are in agreement with TEM images and Ag NPs are confirmed to have a spherical shape.

It was determined from TEM images that nanoparticle sizes change as $AgNO_3$ concentration increased. In the synthesis processes where 1 mM, 2 mM and 4 mM salt concentrations are applied; nanoparticle sizes for thistle seed were found to be 2.5 ± 1 nm, 8 ± 7 nm and 13.5 ± 8.5 nm, respectively.

XRD analysis of Ag NPs

Formation of Ag NPs was confirmed by X-ray diffraction and Ag NPs were interpreted with ICDD (International Center for Diffraction Data) silver library data. Ag NPs exhibit peaks from the surfaces of (111), (200), (220) and (311) in XRD analyzes as specified in ICDD and peak positions are 38.00; 44.21; 64.44 and 77.33, respectively.

In this study, in which green synthesis processes were carried out in accordance with the literature studies, the 2θ values from the surfaces of (111), (200), (220) and (311) belonging to the face centered cubic structure of all Ag NPs were respectively 37.81 ± 0.37; 44.62 ± 0.44; 63.29 ± 0.39; 77.72 ± 0.44. In this state, it is in compliance with the values given in ICDD.

Cytotoxicity studies

In this study, the in vitro cytotoxic effect of Ag NPs produced by green synthesis method was evaluated by MTT test. Ag NPs and MCF-7 cells applied without extract were considered as positive (+) control group. The MTT results showed a significant decrease in the viability of MCF-7 cells at 24 and 48 hours due to the increasing concentration of biosynthesized Ag NPs. According to MTT results, it was calculated as 42 µg/ml after 24 hours of incubation period and 38 µg/ml after 48 hours of incubation.

Similarly, Ag NPs at different mass concentrations have been studied in various studies. IC50 concentrations were calculated in several studies in MCF-7 cell lines. Vivek et al.[39] found the IC50 concentrations of Ag NPs synthesized in *Annona squamosa* extract as 50 µg/ml and 30 µg/ml at the end of 24 and 48 hours' incubation periods, respectively. Similarly, in another study Venugopal et al.[44] stated that the Ag NPs produced using *Syzygium aromaticum* extract had an IC50 concentration of 60 µg/ml after 48 hours of incubation period. Baharara et al.[45] investigated the apoptosis induction in MCF-7 cells through the regulation of bax and bcl-2 gene expression by biosynthesized Ag NPs using extracts of *Achillea biebersteinii* flowers, and they determined the mass concentration dependent cytotoxicity of Ag NPs and detected MCF-7 cell viability that decreased with Ag NP mass concentration. They detected reduced MCF-7 cell viability. Similar processes were followed in this study and it was found that as the concentration of Ag NPs increased, the cell viability of MCF-7 cells decreased, and the IC50 values were calculated to be close to the literature data, as well.

There are studies in the literature in which IC50 values are higher. Farah et al.[46] compared Ag NPs synthesized in *Adenium obesum* extract and the cytotoxicity of purchased Ag NPs on MCF-7 cell lines and found the IC50 value as 217 µg/ml and 73 µg/ml, respectively. The IC50 value of the Ag NPs synthesized with green synthesis method was calculated at a higher mass concentration compared to our study. Similarly, Jyoti et al.[47] investigated the cytotoxicity of Ag NPs that they synthesized in *Picrasma quassioides* leaf extracts against HepG-2 cells and found the IC50 value as 200 µg/ml. Common features of these studies are that IC50 values are higher than many studies. The reason for that may be because they take the mass of Ag NPs as the total mass of extract and $AgNO_3$. Unlike these studies, in our study the experimental processes were completed based on the mass concentrations of Ag ions. We believe that the presented study is compatible with these studies, as our IC50 values were lower.

IC50 values may also vary depending on the plant extracts in which Ag NPs are synthesized. The phytochemicals contained in the plant extracts with the same amount of Ag differ according to each other. Therefore, the cytotoxic effects of milk thistle extracts were also investigated in the study. As shared in the results section, milk thistle extract diluted with 1:1 distilled water was applied on MC-7 cells. These plant extracts alone did not show significant cytotoxic effects at the application concentration.

Cytotoxicity of Ag NPs is affected by the change in particle size. Ag NPs exhibited a vital effect on cell viability, LDH activity[48] and ROS production[49] in a size-dependent manner in different cell lines. It is clear that the surface area, volume ratio and surface reactivity can be changed by particle size.[49–54] In addition, sedimentation rate, mass diffusivity, binding efficiency

and deposition rate of NPs on biological or solid surfaces are significantly affected by particle size.[24,38,50,51]

Particle size can also affect mammalian cell interaction.[24] Various studies have been conducted to determine the particle size effect of Ag NPs on different cell lines.[52–56] Cytotoxic effects of Ag NPs of different sizes have been studied in different studies and different cytotoxic effects have been observed.

In most of the studies, it reflects the hypothesis that smaller particles can cause greater toxicity. To support this statement, Carlson et al.[52] worked with 15 nm and 55 nm hydrocarboncoated Ag NPs and found that 15 nm Ag NPs were able to produce more ROS in a macrophage cell line compared to 55 nm Ag NPs. Using four cell lines (A549, HepG2, MCF-7, SGC7901), Liu et al.[24] found that 5 nm Ag NPs are more toxic than 20 and 50 nm Ag NPs.

In the light of the above-mentioned studies, experimental processes were followed, considering that nanoparticle sizes will affect cytotoxicity. Although size-related cytotoxicity was not investigated in this study, the dimensions of the nanoparticles synthesized in the same plant extracts were determined and the sizes of Ag NPs taken at different concentrations were paid attention to be similar.

Radio-sensitizing effects

Fathy[57] applied X-rays with 400 MU/min and 6 MV energy to MDA-MB-231 cells incubated with Ag NPs at concentrations of 5-10-15-20-25 µg/ml. It was showed in the study that the radio-sensitizing effects of Ag NPs increased depending on the concentrations of Ag NPs.

Lui et al.[58] showed that Ag NPs can be effective on glioma cells. They showed that malignant tumors treated with Ag NPs lead to radiation-induced cytotoxicity. They evaluated the efficacy, safety and radio-sensitizing effects of intratumoral administration of small-sized Ag NPs in combination with ionizing radiation at MV energies for radiation therapy treatment of C6 glioma-bearing rats.

Jyoti et al.[47] applied 6 Gy gamma rays to HepG-2 cells they incubated for 1, 2 and 3 hours with Ag NPs synthesized in *Picrasma quassioides* leaf extracts at the IC50 concentration. In their study, they showed that the surviving fraction was sharply reduced with a gamma radiation dose of 6 Gy. In a similar study, Liu et al.[59] stated that Ag NPs may have radio-sensitizing effects against U251 glioblastoma cells.

Elshawy et al.[60] investigated the radio-sensitizing effects of Ag NPs that they synthesized using *Penicillium aurantiogresium*, a type of plant pathogen, on MCF-7 cells. They stated that the use of Ag NPs in the treatment of MCF-7 cells at the IC50 concentration they determined increased the effect of radiation dose (6 Gy) through inhibition of cell proliferation, activation of lactate dehydrogenase (LDH) and caspase-3.

In the literature, the radio-sensitizing effects of Ag NPs have been studied in limited numbers. In this thesis, Ag NPs were also synthesized in thistle seed extract. Radio-sensitizing effects of Ag NPs synthesized using SM seeds were investigated for the first time. In this study, MCF-7 cells incubated with Ag NPs for 1-2 and 4 hours were exposed to X-ray radiation and cell viability was investigated, and the radio-sensitivity of Ag NPs was evaluated. Similar to the literature data, a radio-sensitizing effect was observed in this study, which was presented depending on the radiation dose.

In this study, IC50 values of Ag NPs synthesized in milk thistle were used as 42 µg/ml. Depending on the radiation dose applied, although the results are almost the same in both IC50 values, they may vary according to the literature data. For example, Elshawy et al.[60] used IC50 concentrations as 10 µg/ml in their study. There are differences between this thesis and IC50 concentrations. As Fathy[57] shows, application doses of Ag NPs taken at different mass concentrations can affect radio-sensitization, so depending on the amount of Ag NP, the radio-sensitivity of the cells may change.

Conclusions

In this study, Ag NPs were obtained after adding 4-2 and 1 mM $AgNO_3$ solution in a ratio of 1:1 to the solutions obtained from the aqueous extracts of thistle seed and mixing in the dark for 24 hours. The obtaining of nanoparticles was verified by UV-Vis Spectrophotometer. According to the UV-vis results, peak maximums vary between 391-423 nm. As a result of XRD examinations, it was determined that all nanoparticles have a face centered cubic crystal lattice. It was determined by TEM images that Ag NPs have a spherical structure and they are compatible with XRD results. Nanoparticle diameters vary between $2.5 \pm 1 - 13.5 \pm 8.5$ nm, and the smallest Ag NP sizes were obtained from a 1 mM $AgNO_3$- thistle seed mixture, and the NP sizes were 2.5 ± 1 nm.

Synthesis of Ag NPs was carried out in accordance with literature examples and different concentrations of synthesized Ag NPs were applied to MCF-7 cells. Ag NPs synthesized with milk thistle taken in equal concentrations with the literature samples showed concentration dependent cytotoxicity against MCF-7 cells.

Radio-sensitizations of Ag NPs were obtained by exposure to 6 Gy X-ray radiation. It was observed that MCF-7 cells incubated with Ag NPs significantly decreased cell viability after exposure to radiation. In radiation studies where only milk thistle extract is applied; It was concluded that the thistle extract had a negligible radio-protective effect. In addition, after 1, 2 and 4 hours of incubation with Ag NPs, a difference was observed in the cytotoxicity of the irradiated cells after 24 hours. However, no data could be obtained on how the exposure of radiation doses to incubated MCF-7 cells affects cytotoxicity.

In this study, green synthesis methods were adopted, and aqueous solutions of milk thistle seeds were preferred as encapsulating and reducing agents during the synthesis process. The cytotoxicity of the obtained Ag NPs in MCF-7 cells was determined and their radio-sensitizing effects were examined. These nanoparticles, whose radio-sensitizing effects have been demonstrated, are preferable with their low cost in the synthesis process. In addition, the fact that milk thistle and its phytochemicals have been widely

researched in the literature is an advantage in terms of reducing the complications of plants and phytochemicals used in the synthesis process.

Plants, with both low cost and rich phytochemical properties are important synthesis agents. It is important to investigate nanoparticles using phytochemicals that are not yet discovered or whose positive aspects are well known, in cancer treatment. More studies are needed on the use of nanoparticles obtained by green synthesis method in cancer treatment.

References

1. Ishikawa, Y.; Shibata, N.; Fukatsu, S. Highly Oriented Si Nanoparticles in SiO2 Created by Si Molecular Beam Epitaxy with Oxygen Implantation. *Thin Solid Films* **1997**, *294*, 227–230. DOI: 10.1016/S0040-6090(96)09215-2.
2. Schmid, G. (Ed.). *Nanoparticles: From Theory to Application*. Hoboken: John Wiley & Sons; **2011**.
3. Ahmad, A.; Senapati, S.; Khan, M. I.; Kumar, R.; Sastry, M. Extracellular Biosynthesis of Monodisperse Gold Nanoparticles by a Novel Extremophilic Actinomycete, Thermomonospora sp. *Langmuir* **2003**, *19*, 3550–3553. [Database] DOI: 10.1021/la026772l.
4. Kowshik, M.; Ashtaputre, S.; Kharrazi, S.; Vogel, W.; Urban, J.; Kulkarni, S. K.; Paknikar, K. M. Extracellular Synthesis of Silver Nanoparticles by a Silver-Tolerant Yeast Strain MKY3. *Nanotechnology* **2003**, *14*, 95–100. DOI: 10.1088/0957-4484/14/1/321.
5. Nasar, S.; Murtaza, G.; Mehmood, A.; Bhatti, T. M.; Raffi, M. Environmentally Benign and Economical Phytofabrication of Silver Nanoparticles Using juglans regia Leaf Extract for Antibacterial Study. *J. Elec. Mater.* **2019**, *48*, 3562–3569. DOI: 10.1007/s11664-019-07109-6.
6. Ozgen, A.; Bilgic, E.; Aydin, S. G.; Nizamlioglu, M. Characterization of Biosynthesized Silver Nanoparticles Using Hypericum Perforatum Leaf and Determination of Their Antibacterial Activity. *Medicine* **2019**, *8*, 503–507. DOI: 10.5455/medscience.2018.07.8985.
7. Krishnakumar, K.; Dineshkumar, B.; Ramesh, P. R. Green Synthesis of Silver Nanoparticles Using Hydnocarpus Pentandra Leaf Extract: In-Vitro Cyto-Toxicity Studies against MCF-7 Cell Line. *J. Young Pharmacists* **2018**, *10*, 16. DOI: 10.5530/jyp.2018.10.5.
8. Arya, G.; Kumari, R. M.; Sharma, N.; Gupta, N.; Kumar, A.; Chatterjee, S.; Nimesh, S. Catalytic, Antibacterial and Antibiofilm Efficacy of Biosynthesised Silver Nanoparticles Using Prosopis Juliflora Leaf Extract along with Their Wound Healing Potential. *J. Photochem. Photobiol. B.* **2019**, *190*, 50–58. DOI: 10.1016/j.jphotobiol.2018.11.005.
9. Valsalam, S.; Agastian, P.; Arasu, M. V.; Al-Dhabi, N. A.; Ghilan, A.-K. M.; Kaviyarasu, K.; Ravindran, B.; Chang, S. W.; Arokiyaraj, S. Rapid Biosynthesis and Characterization of Silver Nanoparticles from the Leaf Extract of Tropaeolum Majus L. and Its Enhanced in-Vitro Antibacterial, Antifungal, Antioxidant and Anticancer Properties. *J. Photochem. Photobiol. B.* **2019**, *191*, 65–74. DOI: 10.1016/j.jphotobiol.2018.12.010.
10. Krishnaraj, C.; Jagan, E. G.; Rajasekar, S.; Selvakumar, P.; Kalaichelvan, P. T.; Mohan, N. J. C. S. B. B. Synthesis of Silver Nanoparticles Using Acalypha Indica Leaf Extracts and Its Antibacterial Activity against Water Borne Pathogens. *Colloids Surf. B. Biointerfaces* **2010**, *76*, 50–56. DOI: 10.1016/j.colsurfb.2009.10.008.
11. Nabikhan, A.; Kandasamy, K.; Raj, A.; Alikunhi, N. M. Synthesis of Antimicrobial Silver Nanoparticles by Callus and Leaf Extracts from Saltmarsh Plant, Sesuvium Portulacastrum L. *Colloids Surf. B. Biointerfaces* **2010**, *79*, 488–493. DOI: 10.1016/j.colsurfb.2010.05.018.
12. Elechiguerra, J. L.; Burt, J. L.; Morones, J. R.; Camacho-Bragado, A.; Gao, X.; Lara, H. H.; Yacaman, M. J. Interaction of Silver Nanoparticles with HIV-1. *J. Nanobiotechnology.* **2005**, *3*, 6. DOI: 10.1186/1477-3155-3-6.
13. Trefry, J. C.; Wooley, D. P. Rapid Assessment of Antiviral Activity and Cytotoxicity of Silver Nanoparticles Using a Novel Application of the Tetrazolium-Based Colorimetric Assay. *J. Virol. Methods* **2012**, *183*, 19–24. DOI: 10.1016/j.jviromet.2012.03.014.
14. Lu, L.; Sun, R. W.-Y.; Chen, R.; Hui, C.-K.; Ho, C.-M.; Luk, J. M.; Lau, G. K. K.; Che, C.-M. Silver Nanoparticles Inhibit Hepatitis B Virus Replication. *Antivir. Ther.* **2008**, *13*, 253–262.
15. Baram-Pinto, D.; Shukla, S.; Perkas, N.; Gedanken, A.; Sarid, R. Inhibition of Herpes Simplex Virus Type 1 Infection by Silver Nanoparticles Capped with Mercaptoethane Sulfonate. *Bioconjug. Chem.* **2009**, *20*, 1497–1502. DOI: 10.1021/bc900215b.
16. Sun, L.; Singh, A. K.; Vig, K.; Pillai, S. R.; Singh, S. R. Silver Nanoparticles Inhibit Replication of Respiratory Syncytial Virus. *J. Biomed. Nanotechnol.* **2008**, *4*, 149–158. DOI: 10.1166/jbn.2008.012.
17. Rogers, J. V.; Parkinson, C. V.; Choi, Y. W.; Speshock, J. L.; Hussain, S. M. A Preliminary Assessment of Silver Nanoparticle Inhibition of Monkeypox Virus Plaque Formation. *Nanoscale Res. Lett.* **2008**, *3*, 129–133. DOI: 10.1007/s11671-008-9128-2.
18. Speshock, J. L.; Murdock, R. C.; Braydich-Stolle, L. K.; Schrand, A. M.; Hussain, S. M. Interaction of Silver Nanoparticles with Tacaribe Virus. *J. Nanobiotechnol.* **2010**, *8*, 19. DOI: 10.1186/1477-3155-8-19.
19. Mehrbod, P.; Motamed, N.; Tabatabaeian, M.; Soleymani Estiar, R.; Amini, E.; Shahidi, M.; Kheyri, M. T. In Vitro Antiviral Effect of "Nanosilver" on Influenza Virus. *Daru J. Pharmaceutical Sci.* **2009**, *17*, 88–93.
20. Xiang, D. X.; Chen, Q.; Pang, L.; Zheng, C. L. Inhibitory Effects of Silver Nanoparticles on H1N1 Influenza a Virus in Vitro. *J. Virol. Methods.* **2011**, *178*, 137–142. DOI: 10.1016/j.jviromet.2011.09.003.
21. Lara, H. H.; Ayala-Nuñez, N. V.; Ixtepan-Turrent, L.; Rodriguez-Padilla, C. Mode of Antiviral Action of Silver Nanoparticles against HIV-1. *J. Nanobiotechnology.* **2010**, *8*, 1–10. DOI: 10.1186/1477-3155-8-1.
22. Sharma, N.; Arya, G.; Kumari, R. M.; Gupta, N.; Nimesh, S. Evaluation of Anticancer Activity of Silver Nanoparticles on the A549 Human Lung Carcinoma Cell Lines through Alamar Blue Assay. *Bio. Protoc.* **2019**, *9*, e3131. DOI: 10.21769/BioProtoc.3131.
23. Jiao, Z. H.; Li, M.; Feng, Y. X.; Shi, J. C.; Zhang, J.; Shao, B. Hormesis Effects of Silver Nanoparticles at Non-Cytotoxic Doses to Human Hepatoma Cells . *PloS One.* **2014**, *9*, e102564. DOI: 10.1371/journal.pone.0102564.
24. Liu, W.; Wu, Y.; Wang, C.; Li, H. C.; Wang, T.; Liao, C. Y.; Cui, L.; Zhou, Q. F.; Yan, B.; Jiang, G. B. Impact of Silver Nanoparticles on Human Cells: Effect of Particle Size. *Nanotoxicology* **2010**, *4*, 319–330. DOI: 10.3109/17435390.2010.483745.
25. Kaba, S. I.; Egorova, E. M. In Vitro Studies of the Toxic Effects of Silver Nanoparticles on HeLa and U937 Cells. *Nanotechnol. Sci. Appl.* **2015**, *8*, 19–29. DOI: 10.2147/NSA.S78134.
26. Scherer, M. D.; Sposito, J. C. V.; Falco, W. F.; Grisolia, A. B.; Andrade, L. H. C.; Lima, S. M.; Machado, G.; Nascimento, V. A.; Gonçalves, D. A.; Wender, H.; et al. Cytotoxic and Genotoxic Effects of Silver Nanoparticles on Meristematic Cells of Allium Cepa Roots: A Close Analysis of Particle Size Dependence. *Sci. Total Environ.* **2019**, *660*, 459–467. DOI: 10.1016/j.scitotenv.2018.12.444.
27. Wu, M.; Guo, H.; Liu, L.; Liu, Y.; Xie, L. Size-Dependent Cellular Uptake and Localization Profiles of Silver Nanoparticles. *Int. J. Nanomedicine.* **2019**, *14*, 4247–4259. DOI: 10.2147/IJN.S201107.
28. Fehaid, A.; Taniguchi, A. Size-Dependent Effect of Silver Nanoparticles on the Tumor Necrosis Factor α-Induced DNA Damage Response. *IJMS.* **2019**, *20*, 1038. DOI: 10.3390/ijms20051038.

29. Shah, M.; Nawaz, S.; Jan, H.; Uddin, N.; Ali, A.; Anjum, S.; Giglioli-Guivarc'h, N.; Hano, C.; Abbasi, B. H. Synthesis of Bio-Mediated Silver Nanoparticles from Silybum Marianum and Their Biological and Clinical Activities. *Mater. Sci. Eng. C. Mater. Biol. Appl.* **2020**, *112*, 110889. DOI: 10.1016/j.msec.2020.110889.
30. Ramasamy, K.; Agarwal, R. Multitargeted Therapy of Cancer by Silymarin. *Cancer Lett.* **2008**, *269*, 352–362. DOI: 10.1016/j.canlet.2008.03.053.
31. Zhao, Y.; Chen, B.; Yao, S. Simultaneous Determination of Abietane-Type Diterpenes, Flavonolignans and Phenolic Compounds in Compound Preparations of Silybum Marianum and Salvia Miltiorrhiza by HPLC-DAD-ESI MS. *J. Pharm. Biomed. Anal.* **2005**, *38*, 564–570. DOI: 10.1016/j.jpba.2005.01.021.
32. Flora, K.; Hahn, M.; Rosen, H.; Benner, K. Milk Thistle (Silybum Marianum) for the Therapy of Liver Disease. *Am. J. Gastroenterol.* **1998**, *93*, 139–143. DOI: 10.1016/S0002-9270(97)00082-8
33. Fanoudi, S.; Alavi, M. S.; Karimi, G.; Hosseinzadeh, H. Milk Thistle (*Silybum marianum*) as an Antidote or a Protective Agent against Natural or Chemical Toxicities: A Review. *Drug Chem. Toxicol.* **2020**, *43*, 240–254. DOI: 10.1080/01480545.2018.1485687.
34. Tzeng, J. I.; Chen, M. F.; Chung, H. H.; Cheng, J. T. Silymarin Decreases Connective Tissue Growth Factor to Improve Liver Fibrosis in Rats Treated with Carbon Tetrachloride. *Phytother. Res.* **2013**, *27*, 1023–1028. DOI: 10.1002/ptr.4829.
35. Shaker, E.; Mahmoud, H.; Mnaa, S. Silymarin, the Antioxidant Component and Silybum Marianum Extracts Prevent Liver Damage. *Food Chem. Toxicol.* **2010**, *48*, 803–806. DOI: 10.1016/j.fct.2009.12.011.
36. Bhatia, N.; Zhao, J.; Wolf, D. M.; Agarwal, R. Inhibition of Human Carcinoma Cell Growth and DNA Synthesis by Silibinin, an Active Constituent of Milk Thistle: Comparison with Silymarin. *Cancer Lett.* **1999**, *147*, 77–84. DOI: 10.1016/S0304-3835(99)00276-1.
37. Henglein, A. Small-Particle Research: physicochemical Properties of Extremely Small Colloidal Metal and Semiconductor Particles. *Chem. Rev.* **1989**, *89*, 1861–1873. DOI: 10.1021/cr00098a010.
38. Sharma, V. K.; Yngard, R. A.; Lin, Y. Silver Nanoparticles: green Synthesis and Their Antimicrobial Activities. *Adv. Colloid Interface Sci.* **2009**, *145*, 83–96. DOI: 10.1016/j.cis.2008.09.002.
39. Vivek, R.; Thangam, R.; Muthuchelian, K.; Gunasekaran, P.; Kaveri, K.; Kannan, S. Green Biosynthesis of Silver Nanoparticles from Annona Squamosa Leaf Extract and Its in Vitro Cytotoxic Effect on MCF-7 Cells. *Process Biochem.* **2012**, *47*, 2405–2410. DOI: 10.1016/j.procbio.2012.09.025.
40. Elemike, E. E.; Onwudiwe, D. C.; Nundkumar, N.; Singh, M.; Iyekowa, O. Green Synthesis of Ag, Au and Ag-Au Bimetallic Nanoparticles Using Stigmaphyllon Ovatum Leaf Extract and Their in Vitro Anticancer Potential. *Mater. Lett.* **2019**, *243*, 148–152. DOI: 10.1016/j.matlet.2019.02.049.
41. Kumar, V.; Yadav, S. K. Plant-Mediated Synthesis of Silver and Gold Nanoparticles and Their Applications. *J. Chem. Technol. Biotechnol.* **2009**, *84*, 151–157. DOI: 10.1002/jctb.2023.
42. Mie, G. Beiträge Zur Optik Trüber Medien, Speziell Kolloidaler Metallösungen. *Ann. Phys.* **1908**, *330*, 377–445. DOI: 10.1002/andp.19083300302.
43. He, R.; Qian, X.; Yin, J.; Zhu, Z. Preparation of Polychrome Silver Nanoparticles in Different Solvents. *J. Mater. Chem.* **2002**, *12*, 3783–3786. DOI: 10.1039/b205214h.
44. Venugopal, K.; Rather, H. A.; Rajagopal, K.; Shanthi, M. P.; Sheriff, K.; Illiyas, M.; Rather, R. A.; Manikandan, E.; Uvarajan, S.; Bhaskar, M.; Maaza, M. Synthesis of Silver Nanoparticles (Ag NPs) for Anticancer Activities (MCF 7 Breast and A549 Lung Cell Lines) of the Crude Extract of Syzygium aromaticum. *J. Photochem. Photobiol. B.* **2017**, *167*, 282–289. DOI: 10.1016/j.jphotobiol.2016.12.013.
45. Baharara, J.; Namvar, F.; Ramezani, T.; Hosseini, N.; Mohamad, R. Green Synthesis of Silver Nanoparticles Using Achillea Biebersteinii Flower Extract and Its anti-Angiogenic Properties in the Rat Aortic Ring Model. *Molecules* **2014**, *19*, 4624–4634. DOI: 10.3390/molecules19044624.
46. Farah, M. A.; Ali, M. A.; Chen, S.-M.; Li, Y.; Al-Hemaid, F. M.; Abou-Tarboush, F. M.; Al-Anazi, K. M.; Lee, J. Silver Nanoparticles Synthesized from Adenium Obesum Leaf Extract Induced DNA Damage, Apoptosis and Autophagy via Generation of Reactive Oxygen Species. *Colloids Surf, B.* **2016**, *141*, 158–169. DOI: 10.1016/j.colsurfb.2016.01.027.
47. Jyoti, K.; Singh, A.; Fekete, G.; Singh, T. Cytotoxic and Radiosensitizing Potential of Silver Nanoparticles against HepG-2 Cells Prepared by Biosynthetic Route Using Picrasma Quassioides Leaf Extract. *J. Drug Delivery Sci. Technol.* **2020**, *55*, 101479. DOI: 10.1016/j.jddst.2019.101479.
48. Carlson, C.; Hussain, S. M.; Schrand, A. M. K.; Braydich-Stolle, L.; Hess, K. L.; Jones, R. L.; Schlager, J. J. Unique Cellular Interaction of Silver Nanoparticles: size-Dependent Generation of Reactive Oxygen Species. *J. Phys. Chem. B.* **2008**, *112*, 13608–13619. DOI: 10.1021/jp712087m.
49. Chen, S. F.; Zhang, H. Aggregation Kinetics of Nanosilver in Different Water Conditions. *Adv. Nat. Sci: Nanosci. Nanotechnol.* **2012**, *3*, 035006. DOI: 10.1088/2043-6262/3/3/035006.
50. Jiang, Z. J.; Liu, C. Y.; Sun, L. W. Catalytic Properties of Silver Nanoparticles Supported on Silica Spheres. *J. Phys. Chem. B.* **2005**, *109*, 1730–1735. DOI: 10.1021/jp046032g.
51. Petosa, A. R.; Jaisi, D. P.; Quevedo, I. R.; Elimelech, M.; Tufenkji, N. Aggregation and Deposition of Engineered Nanomaterials in Aquatic Environments: role of Physicochemical Interactions. *Environ. Sci. Technol.* **2010**, *44*, 6532–6549. DOI: 10.1021/es100598h.
52. Sriram, M. I.; Kalishwaralal, K.; Barathmanikanth, S.; Gurunathani, S. Size-Based Cytotoxicity of Silver Nanoparticles in Bovine Retinal Endothelial Cells. *Nanoscience Methods* **2012**, *1*, 56–77. DOI: 10.1080/17458080.2010.547878.
53. Park, E. J.; Yi, J.; Kim, Y.; Choi, K.; Park, K. Silver Nanoparticles Induce Cytotoxicity by a Trojan-Horse Type Mechanism. *Toxicol In Vitro.* **2010**, *24*, 872–878. DOI: 10.1016/j.tiv.2009.12.001.
54. Lankoff, A.; Sandberg, W. J.; Wegierek-Ciuk, A.; Lisowska, H.; Refsnes, M.; Sartowska, B.; Schwarze, P. E.; Meczynska-Wielgosz, S.; Wojewodzka, M.; Kruszewski, M. The Effect of Agglomeration State of Silver and Titanium Dioxide Nanoparticles on Cellular Response of HepG2, A549 and THP-1 Cells. *Toxicol. Lett.* **2012**, *208*, 197–213. DOI: 10.1016/j.toxlet.2011.11.006.
55. Le, A. T.; Huy, P. T.; Tam, P. D.; Huy, T. Q.; Cam, P. D.; Kudrinskiy, A. A.; Krutyakov, Y. A. Green Synthesis of Finely-Dispersed Highly Bactericidal Silver Nanoparticles via Modified Tollens Technique. *Curr. Appl. Phys.* **2010**, *10*, 910–916. DOI: 10.1016/j.cap.2009.10.021.
56. Arora, S.; Jain, J.; Rajwade, J. M.; Paknikar, K. M. Interactions of Silver Nanoparticles with Primary Mouse Fibroblasts and Liver Cells. *Toxicol. Appl. Pharmacol.* **2009**, *236*, 310–318. DOI: 10.1016/j.taap.2009.02.020.
57. Fathy, M. M. Biosynthesis of Silver Nanoparticles Using Thymoquinone and Evaluation of Their Radio-Sensitizing Activity. *Bionanosci.* **2020**, *10*, 260–267. DOI: 10.1007/s12668-019-00702-3.
58. Liu, P.; Huang, Z.; Chen, Z.; Xu, R.; Wu, H.; Zang, F.; Wang, C.; Gu, N. Silver Nanoparticles: A Novel Radiation Sensitizer for Glioma? *Nanoscale* **2013**, *5*, 11829–11836. DOI: 10.1039/C3NR01351K.
59. Liu, P.; Jin, H.; Guo, Z.; Ma, J.; Zhao, J.; Li, D.; Wu, H.; Gu, N. Silver Nanoparticles Outperform Gold Nanoparticles in Radiosensitizing U251 Cells in Vitro and in an Intracranial Mouse Model of Glioma. *Int. J. Nanomedicine.* **2016**, *11*, 5003–5014. DOI: 10.2147/IJN.S115473.
60. Elshawy, O. E.; Helmy, E. A.; Rashed, L. A. Preparation, Characterization and in Vitro Evaluation of the Antitumor Activity of the Biologically Synthesized Silver Nanoparticles. *ANP.* **2016**, *5*, 149–166. DOI: 10.4236/anp.2016.52017.